CHEMISTRY
A EUROPEAN JOURNAL

DOI: 10.1002/chem.200800021

Synthesis and Properties of DNA Complexes Containing 2,2,6,6-Tetramethyl-1-piperidinoxy (TEMPO) Moieties as Organic Radical Battery Materials

Jinqing Qu,[a, f] Ryuhei Morita,[a] Masaharu Satoh,[b] Jun Wada,[c] Fumiaki Terakura,[d] Kenji Mizoguchi,[d] Naoya Ogata,[e] and Toshio Masuda*[a]

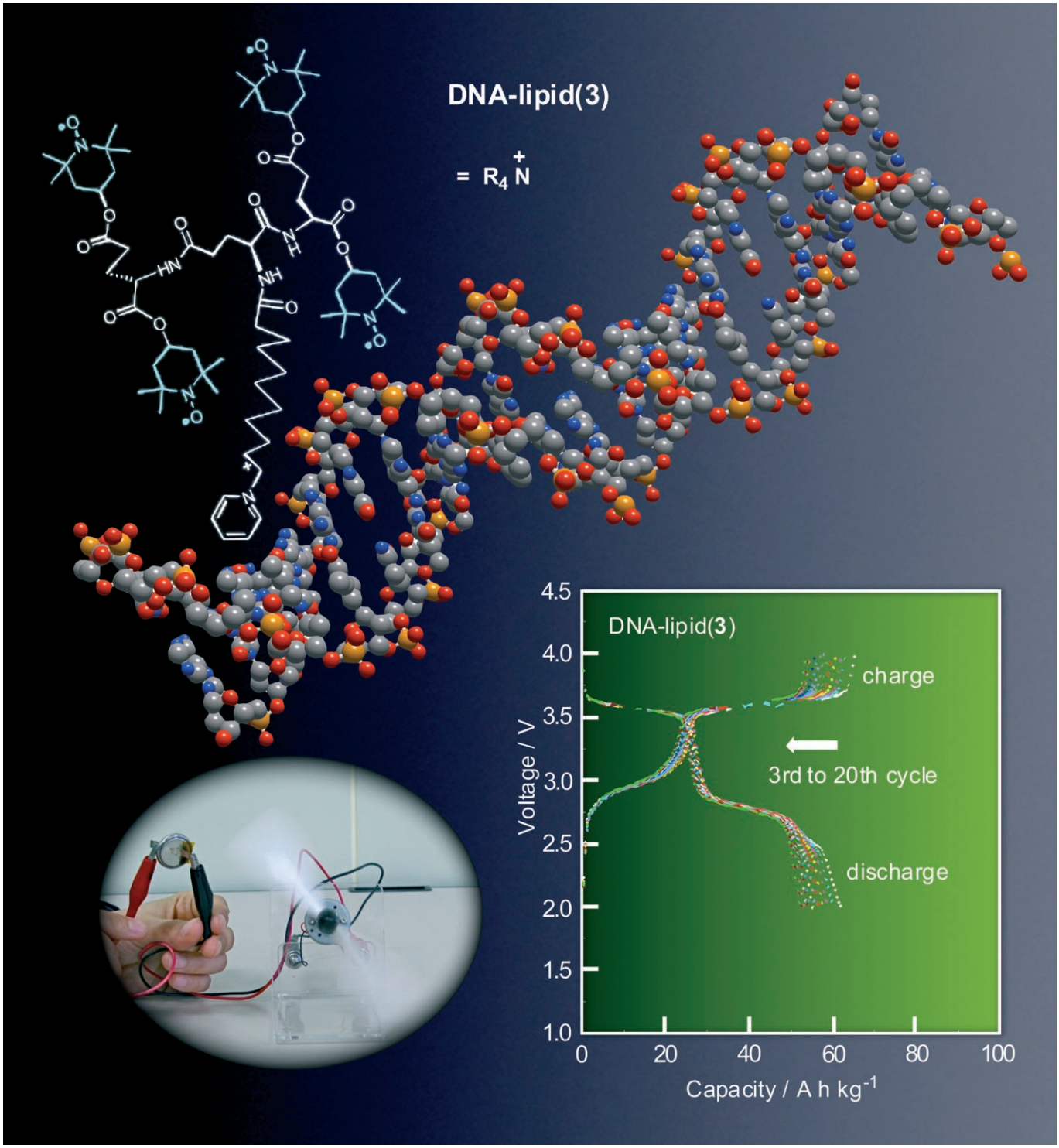

Abstract: We report here the first example of organic radical battery with DNA. Though there is a growing interest in DNA/cationic-lipid complexes as promising gene delivery vehicles, few efforts have been focused on the use of such complexes as advanced materials for organic optoelectronic applications. The present article describes how substitution of the sodium counter cation of DNA with cationic amphiphilic lipid(**1**–**4**) provided novel DNA–lipid complexes that contain TEMPO radicals, in which the actual mole ratio of phosphate to lipid was 1:0.84 to 1:0.16. All the TEMPO-containing DNA–lipid complexes displayed reversible two-stage charge/discharge processes, the discharge capacities of which were 40.5–60.0 A h kg^{-1}. In particular, the capacity of a DNA–lipid(**3**)-based cell reached 60.0 A h kg^{-1}, which corresponds to 192% relative to its theoretical value for the single-electron one-stage process, indicating a two-electron process.

Keywords: batteries · charge/discharge properties · DNA · electrochemistry · lipids · radicals

Introduction

DNA possesses many physical and chemical properties that make it a powerful material for molecular constructions on the nanometer-length scale.[1] Furthermore, DNA is an anionic polyelectrolyte, which can be quantitatively precipitated with cationic surfactants in water to form DNA/cationic-lipid complexes. DNA complexes afford useful nonviral delivery systems as a powerful protocol for gene therapy and vaccination in biotechnology and medical applications. DNA complexes also remind us of the coil-to-globule transition in synthetic polymers, exhibiting intriguing liquid crystalline and polyelectrolyte behavior.[2–4] Much work has been dedicated to revealing supramolecular structures and morphologies in DNA/cationic-lipid complexes, which is primarily stimulated by nonviral gene delivery.[5–10] We think that DNA–lipid complex materials are also promising in applications to optoelectronic materials for the following reasons: First, not only is the electron transfer on DNA mediated by solvated (hydrated) electron, moving along the phosphate backbone,[11] but also DNA conveys electric current as efficiently as a good semiconductor and gives membrane materials of high optical transparency.[12,13] Second, DNA-based materials feature relatively high physicochemical stability, which is much higher than that of proteins. Hence, DNA–lipid complex materials can be synthesized, processed, and stored under a broad range of environmental conditions without the necessity of special precautions to avoid decomposition. Third, the design and synthesis of cationic lipids (liposomes, dendrimers, and polymers) carrying optoelectronic functional groups are well known, and it is easy to prepare complexes of DNA with them to obtain advanced materials with unique electronic and optical properties for potential applications including one-dimensional semiconductors, nonlinear optics, field-effect transistors, and photovoltaics.

On the other hand, 2,2,6,6-tetramethyl-1-piperidinyloxy (TEMPO) and its derivatives are known, stable nitroxy radicals and have found applications in a variety of fields such as spin labels in the study of conformation and structural mobility of biological systems,[14] scavengers of unstable radical species,[15] and oxidizing agents.[16] Polymers carrying TEMPO radicals have been intensively studied in the fields of electron-spin resonance[17] and molecular motion,[18,19] and frequently employed as functional materials, such as polymeric stabilizers[20] and oxidants of alcohols.[21,22] TEMPO-carrying polymers can also be applied to cathode-active materials in secondary batteries, called organic radical batteries. Such batteries possess numerous advantages over lithium-ion batteries, such as large charge and discharge rates and, more importantly, environmentally friendly and safe nature due to the absence of heavy metals.[23–27] We have recently investigated the preparation and charge/discharge properties of several polyacetylenes and polynorbornenes containing TEMPO groups, and revealed that the discharge capacity of certain cells fabricated with polymers carrying TEMPO radicals reaches the theoretical values expected from their molecular structures.[28–30] Thus far, all of the studies about organic radical batteries have been carried out with synthetic polymers.

The present paper deals with the preparation and fundamental properties of DNA–lipid complexes containing TEMPO radicals, and further their charge/discharge charac-

[a] Dr. J. Qu, R. Morita, Prof. Dr. T. Masuda
Department of Polymer Chemistry
Graduate School of Engineering, Kyoto University
Katsura Campus, Kyoto 615-8510 (Japan)
Fax: (+81) 75-383-2590
E-mail: masuda@adv.polym.kyoto-u.ac.jp

[b] Dr. M. Satoh
Murata Manufacturing Co.
Yasu, Shiga, 520–2393 (Japan)

[c] J. Wada
Corporate Planning Department
Nippon Kasei Chemical Co.
1-8-8 Shinkawa, Chuoku, Tokyo 104-0033 (Japan)

[d] F. Terakura, Prof. Dr. K. Mizoguchi
Department of Physics, Tokyo Metropolitan University
Hachi-oji, Tokyo 192-0397 (Japan)

[e] Prof. Dr. N. Ogata
Ogata Research Labotratory
Kashiwa-dai Minami 1-3-1, Chitose 066-0009 (Japan)

[f] Dr. J. Qu
The School of Chemistry and Chemical Engineering
South China University of Technology, Guangzhou, 510640 (China)

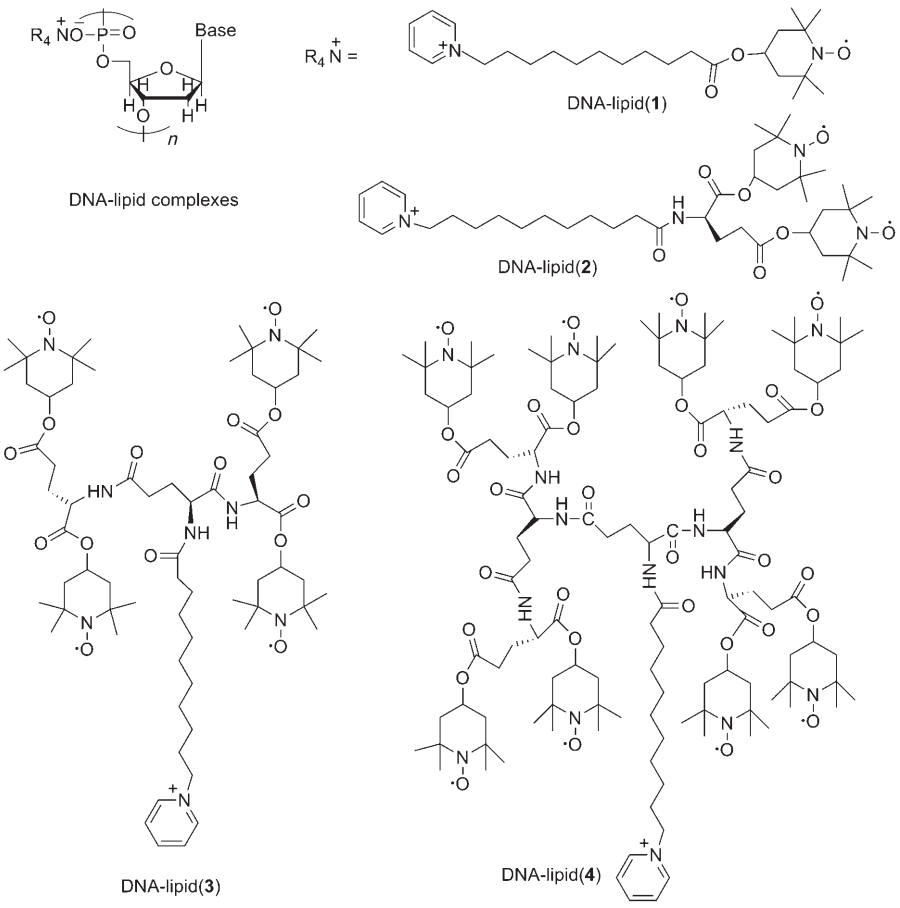

teristics as cathode-active materials in organic radical batteries. To the best of our knowledge, the present research shows the first example of secondary battery with DNA. In general, organic radical batteries as studied here feature high charge speed and large power relative to lithium ion batteries.

Results and Discussion

Synthesis of DNA–lipid complexes: We synthesized at first four cationic lipids carrying TEMPO radicals, lipid(**1**–**4**), and then DNA–lipid(**1**–**4**) in the following way. When an aqueous solution of DNA–Na was added into aqueous lipid solutions, DNA–lipid complexes immediately precipitated from the aqueous solutions. After stirring for 24 h, the white flocculous products were filtered off to provide DNA–lipids with 39–57 % yields. Table 1 summarizes the conditions and results of preparation of the DNA–lipid complexes. These complexes were completely soluble in $CHCl_3$, CH_2Cl_2, methanol, and ethanol, while they were insoluble in water, THF, toluene, diethyl ether, and *n*-hexane. The elemental analyses revealed that the formed DNA–lipid complexes possessed compositions with the phosphate anion to cationic amphiphile ratios of 1:0.84 to 1:0.16 (Table 1).

The ICP (inductively coupled plasma) analyses disclosed that the Na^+ of DNA was almost completely replaced by the cationic lipids. The content of lipid in DNA–lipid(**1**) was as high as about 80 % of its theoretical value, while those in DNA–lipid(**2**–**4**) decreased progressively as the lipids became bulkier. A reason for this finding is that lipid(**2**–**4**) possess amino acid based dendrimer structures that exhibit properties based on both cationic and neutral lipids, whereas the complexation behavior of lipid(**1**), which exhibits only cationic lipid properties, is simpler.[31]

Characterization of the DNA–lipid complexes: Figure 1 depicts the FTIR spectra of DNA–Na, lipid(**1**), lipid(**3**), DNA–lipid(**1**), and DNA–lipid(**3**). The IR spectra of DNA–lipid(**1**–**4**) displayed almost all absorptions characteristic of those in both lipids and DNA–Na. The spectra of DNA–lipid(**1**) and DNA–lipid(**3**) complexes exhibit the absorption bands at 1234 and 1695 cm^{-1} attributable to antisymmetric stretching of PO_2^- and stretching of C=O in the base pairs (thymine (T), guanine (G), and cytosine (C)) of the DNA, respectively, while the bands at 2927 and 2846 cm^{-1} are attributable to the $-CH_3$ and $-CH_2$ stretching of lipid moieties.

All of DNA–lipid(**1**–**4**) showed a large positive circular dichroism (CD) signal at 290 nm and a negative CD signal at 260 nm in $CHCl_3$ in Figure 2, indicating that they adopted a double-helical C-form conformation different from that of

Table 1. Preparation of DNA–lipid complexes containing TEMPO.

Sample	Yield [%][a]	Replacement of Na^+ [%][b]	$R_{l/p}$ Lipid/phosphate [mole ratio][c]	$R_{t/p}$ TEMPO/phosphate [mole ratio][d]
DNA–lipid(**1**)	56	97	0.84	0.84
DNA–lipid(**2**)	57	97	0.57	1.14
DNA–lipid(**3**)	46	96	0.33	1.32
DNA–lipid(**4**)	39	96	0.16	1.28

[a] DNA–lipid complexes were obtained as water-insoluble part. The yields were determined according to Equation (2). [b] Determined by ICP. [c] Calculated according to Equation (4). [d] Determined according to Equation (5).

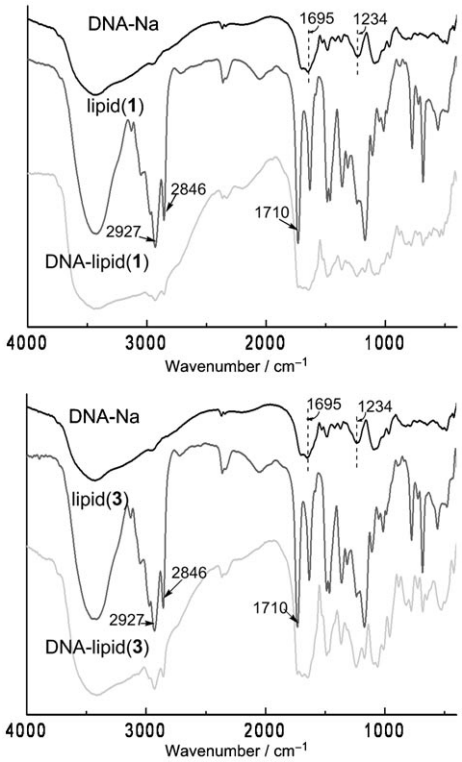

Figure 1. IR spectra of DNA–Na, lipid(**1**), lipid(**3**), DNA–lipid(**1**), and DNA–lipid(**3**) (KBr pellet).

native DNA, which forms a double-helical B-form structure in aqueous solution. The UV/Vis spectra of DNA–lipid(**1**–**4**) exhibited almost the same absorption peaks at 265 nm assignable to the nucleobases, and their CD signals and UV/Vis absorptions were all slightly blue-shifted (5 nm) when the solvent was changed from $CHCl_3$ to methanol. When the measuring temperature was raised from −10 to 40 °C in methanol, the magnitude of Cotton effect decreased. This phenomenon is different from the aqueous DNA–Na solution, which exhibits only slight changes of Cotton effect in a temperature range of 10 to 90 °C. The UV/Vis spectra of DNA–lipid complexes hardly changed in a temperature range of −10 to 40 °C (the figure is not shown). It is considered that the lipids depressed the thermal stability of helical conformation of DNA–lipids.

The onset temperatures of weight loss of DNA–lipid(**1**–**4**) were almost the same and around 220 °C under air according to TGA analyses (Figure 3). All of the DNA–lipid complexes containing TEMPO decomposed in similar fashions; they did not lose weight completely even though temperature was raised up to 900 °C, probably due to the remaining P_2O_5.

The ESR spectra of DNA–lipid(**1**–**4**) at room temperature in the powder state taken with a JEOL JES-FR30 X-band (9.48 GHz) spectrometer exhibited one sharp singlet signal with $g = 2.0067$ to 2.0068; these values are typical of the nitroxy free radicals.[31] A frequency counter (Anritsu, MF76 A) and an NMR field meter (Echo Electronics, EFM-2000 AX) were used for the precise determination of these g factors. The ESR line widths showed a distinct frequency dependence, suggesting a quasi-one-dimensional spin–spin interaction along the 1D DNA double helix.[32] The spin numbers of DNA–lipid(**1**–**4**) in Table 2 were evaluated by two independent methods:

1) A low-frequency ESR-NMR method, in which the ESR and broad-line ^{1}H NMR spectra were taken at the same frequency with varying the magnetic field. The doubly integrated intensity of ESR signals was compared with that of broad-line ^{1}H NMR spectra. The standard ESR sample is not needed to estimate the spin susceptibility, if the number of hydrogen atoms included in the molecular unit is known.
2) The estimation by the Curie constant C of the Curie–Weiss spin susceptibility, $\chi_{spin} = C/(T+\theta)$, measured by a Quantum Design MPMS-07 SQUID magnetometer.

The reasonable agreement of the values obtained by these two methods suggests reliability of the estimations. The average number of spins of the two methods were more or less smaller than that of TEMPO moiety in the lipids except for DNA–lipid(**1**). A possible reason for this is that a part of TEMPO becomes oxidized into the oxoammonium cation.

Figure 4 illustrates the cyclic voltammetry (CV) curves of DNA–lipid(**1**) and DNA–lipid(**3**). DNA–lipid(**3**) exhibits an oxidation potential peak at 0.70 V versus Ag/Ag^+ and a reduction potential peak at 0.45 V versus Ag/Ag^+ when measured at a sweep rate of 0.01 $V s^{-1}$. It is noted that the distance between the oxidation and reduction potential peaks of DNA–lipid(**1**) is 0.25 V, which is much larger than those of polyacetylenes containing TEMPO (ca. 0.070 V), which suggests that the TEMPO moieties linked with DNA through lipids undergo slower redox reactions. The oxidation and reduction peaks of DNA–lipid(**1**) scarcely changed after five CV scans, indicating that the complex is electrochemically quite stable. The CV curves of DNA–lipid(**2**–**4**) were similar to that of DNA–lipid(**1**).

Charge/discharge properties of the DNA–lipid complexes: Figure 5 delineates the charge/discharge curves of the cells fabricated by using DNA–lipid(**1**–**4**) measured at a constant current density of 0.088 $mA cm^{-2}$ (0.0385–0.0452 $A g^{-1}$) in the voltage range of 2.0–4.2 V. During the charge process of DNA–lipid(**3**), voltage sharply increased from 2.0 to 3.5 V in a range of 0–30 $A h kg^{-1}$ cell capacity, followed by a plateau at about 3.5–3.6 V up to a cell capacity of 62 $A h kg^{-1}$, and voltage finally increased to a top cutoff of 4.2 V. Similarly, during the discharge process of DNA–lipid(**3**), voltage quickly reduced from 3.8 to 3.5 V within 0–5 $A h kg^{-1}$ cell capacity, followed by a plateau at about 3.7–3.4 V until the capacity reached 25 $A h kg^{-1}$. Then voltage sharply decreased to 2.7 V, followed by another plateau at about 2.7–2.3 V up to a cell capacity of 60 $A h kg^{-1}$, and voltage then gradually decreased to a bottom cutoff voltage at 2.0 V. It is very interesting and important that the discharge curves of DNA–

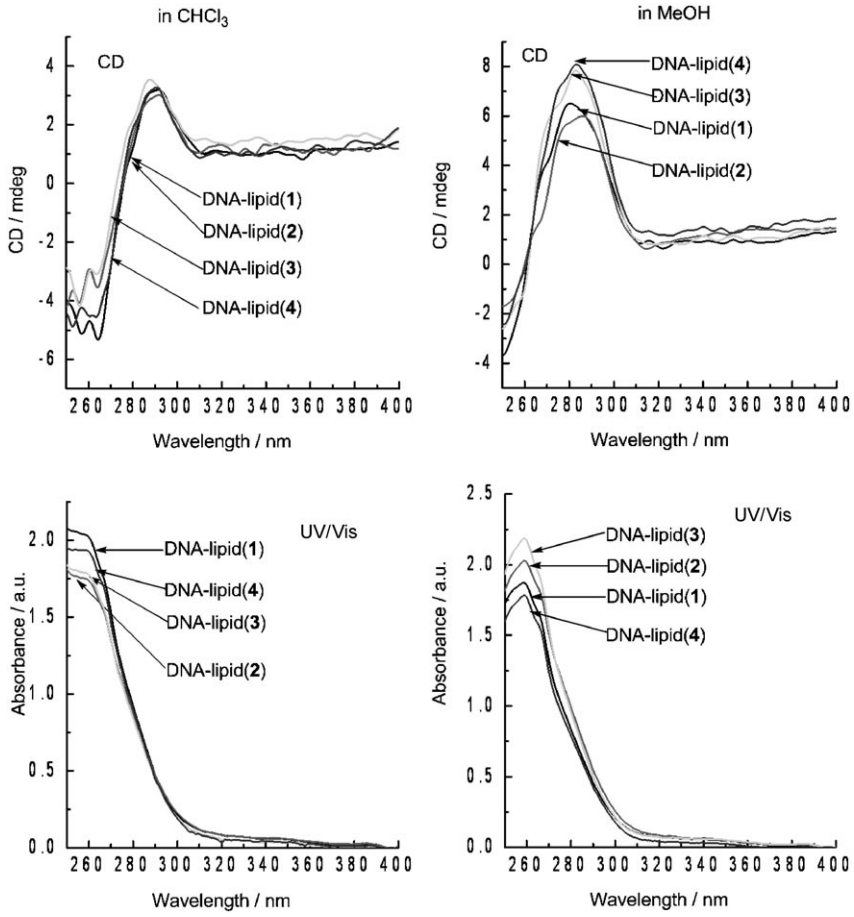

Figure 2. Circular dichroism (CD) and UV/Vis spectra of DNA–lipid(**1**–**4**) measured in $CHCl_3$ and methanol at 22 °C (sample concentration: 0.05 mg mL^{-1}).

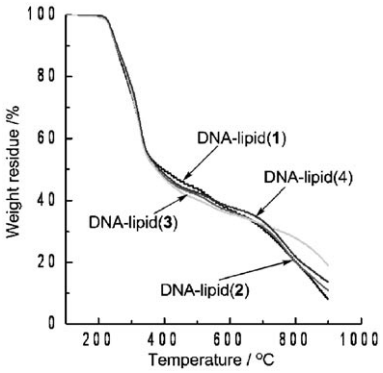

Figure 3. TGA curves of DNA–lipid(**1**–**4**) measured at a heating rate of 10 °C min^{-1} in air.

lipid(**3**) displays two voltage plateaus, one in the range of 3.4–3.7 V and the second one in the range of 2.3–2.7 V; the first voltage corresponds to the redox potential between the TEMPO radical and cation. The charge/discharge process of the other DNA–lipid cmplexes behaved similarly to that of DNA–lipid(**3**). Thus, all of the present complexes exhibit clear voltage plateaus at about 3.6 and 2.5 V in discharge curves, indicating that the polymers can be used as cathode-active materials of a rechargeable battery.

Figure 6 depicts the charge/discharge curves of DNA–lipid(**1**) and DNA–lipid(**3**) at 0.0385 A g^{-1} current density in a range of 2.0–4.0 V cell voltage and at which charge and discharge were repeated for 20 cycles. The charge/discharge curves of DNA–lipid(**1**) do not change very much during from the 1st to 20th cycle, showing that the DNA–lipid possess stable charge/discharge properties. It is reasonable to assume the following: 1) the charge process at cathode is the oxidation of TEMPO in the polymers from **5** to oxoammonium salt **6**, for which the charge capacity at the 1st stage in the first cycle is about 18 A h kg^{-1} (Figure 6); 2) the discharge process is a two-stage reduction process, namely, the first reduction of salt **6** to form **5** in which the discharge capacity at 1st stage is about 29.0 A h kg^{-1}, and further reduction of **5** to form **7** in which the discharge capacity at 2nd stage is about 31.0 A h kg^{-1}; 3) the second charge process begins from **7** to **6** [Eq. (1)], the charge capacity at 2nd stage is about 42 A h kg^{-1}, and the charge/discharge capacity is slightly reduced during the 2nd to 20th cycles. Figure 6 clearly displays a two-stage charge/discharge process. The above-stated results present the first clear example that a TEMPO-based cathode-active material exhibits a two-stage redox reaction from a cation via a radical to an anion. This two-stage reaction is useful to achieve high capacity, because the capacity doubles. If this generally holds, such batteries should be rather called organic ion batteries instead of organic radical batteries. The charging/discharging properties of lipids that contain TEMPO radicals as controlled experiments were similar to those of our previously reported polymers including polynorborene and polyacetylenes that contain TEMPO radicals.[28–30]

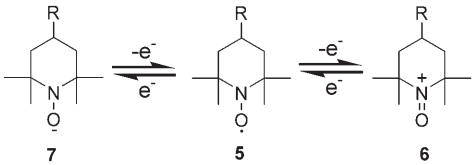

(1)

Table 2. ESR data of DNA–lipid complexes.

	ESR g factor	ESR line width [G][a] ≈50 MHz	≈9.4 GHz	D_S [10^{21} spin g^{-1}]	N_S [spin per unit] By SQUID[b]	By ESR	$\langle N_S \rangle$ average	$R_{r/p}$ TEMPO radical/ phosphate [mole ratio][c]
DNA–lipid(**1**)	2.0068	24.3	15.5	0.76	0.85	1.05	0.95	0.80
DNA–lipid(**2**)	2.0067	23.6	13.1	0.69	1.34	1.53	1.43	0.82
DNA–lipid(**3**)	2.0068	23.6	13.3	0.70	2.57	2.62	2.60	0.86
DNA–lipid(**4**)	2.0067	23.0	13.0	0.73	5.30	5.46	5.38	0.86

[a] This frequency dependence of ESR spectra could be attributed to the one-dimensional spin–spin interaction along DNA double helix. [b] Calculated according to Equation (6) with the actual molecular weight M defined by Equation (7). [c] Calculated according to Equation (8).

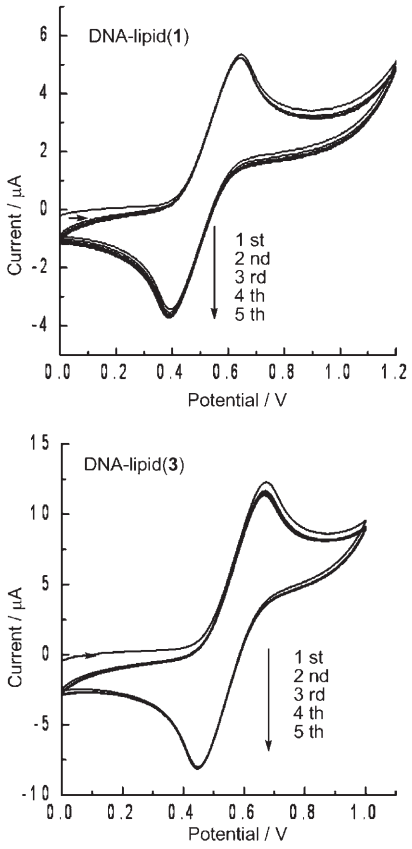

Figure 4. Cyclic voltammograms (CV) of DNA–lipid(**1**) and DNA–lipid(**3**) measured at a scan rate of 0.01 V s^{-1} versus Ag/Ag^+ in TBAP solution.

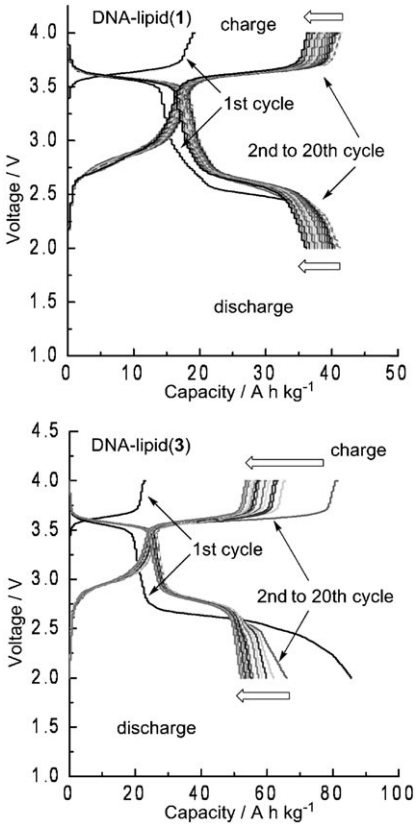

Figure 6. Charge/discharge curves of DNA–lipid(**1**) and DNA–lipid(**3**) at a current density of 0.088 mA cm^{-2} (0.0385 A g^{-1}) in a range of 2.0–4.0 V cell voltage in 20 cycles.

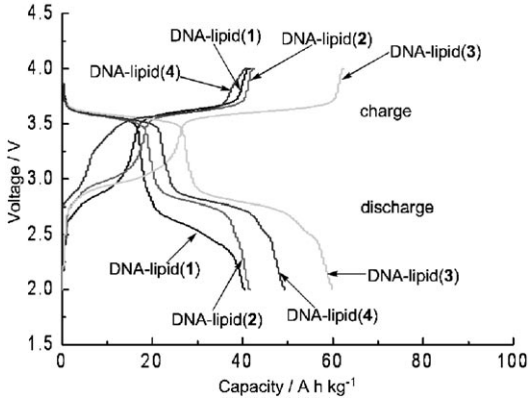

Figure 5. Charge-discharge curves of DNA–lipid(**1**–**4**) at a current density of 0.088 mA cm^{-2} (0.0385–0.0452 A g^{-1}) in a range of 2.0–4.2 V cell voltage. The third cycle is depicted.

Taking it into account that one TEMPO moiety provides one electron in the first-stage redox process, we can estimate the theoretical capacities of the cells by taking DNA–lipid(**1**–**4**) to be 30.7–32.7 A h kg^{-1} (Table 3). Evaluating from the values at 2.0 V in Figure 5, the initial discharge capacities of these cells are determined to be 40.5–60.0 A h kg^{-1} per complex weight at a current density of 0.088 mA cm^{-2} (0.0385–0.0452 A g^{-1}). In particular, the observed discharge capacity of DNA–lipid(**3**) reached 60.0 A h kg^{-1}, which corresponds to 192% of the theoretical capacity for the one-electron redox reaction. This demonstrates that DNA–lipid(**3**) displays a high capacity that can lead to a wide range of potential applications as a power source. On the other hand, the capacities of the DNA–lipid(**1**)-, DNA–lipid(**2**)- and DNA–lipid(**4**)-based cells remained 40.5, 41.7, and 49.2 A h kg^{-1}, respectively (Table 3), and lower than that of the DNA–

Table 3. Capacity data of DNA–lipid complexes.

	C_{th} Theoretical capacity [A h kg^{-1}][a]	Observed capacity [A h kg^{-1}]			Observed capacity/theoretical capacity [%]		
		1st stage[b]	2nd stage[c]	total	1st stage	2nd stage	total
DNA–lipid(**1**)	32.7	18.1	22.4	40.5	55	69	124
DNA–lipid(**2**)	30.7	20.8	20.9	41.7	68	68	136
DNA–lipid(**3**)	31.2	29.0	31.0	60.0	93	99	192
DNA–lipid(**4**)	32.5	24.0	25.2	49.2	74	76	150

[a] Calculated according to Equation (9). [b] Discharge capacity in the third cycle at a current density of 0.088 mA cm^{-2} (0.0385–0.0452 A g^{-1}) and a cut-off at 3.0 V. [c] Discharge capacity in the third cycle at a current density of 0.088 mA cm^{-2} (0.0385–0.0452 A g^{-1}) and a cut-off at 2.0 V.

lipid(**3**)-based counterpart. This seems to be due to differences in both molecular structures (e.g., spacial arrangement of the TEMPO radicals) and macroscopic aggregation states (e.g., the size and hardness of particles of polymer materials).

Figure 7 illustrates the cycle performance of the DNA–lipid(**1**–**4**)/Li cells, in which charge and discharge were repeated at 0.88 mA cm^{-2} (0.385–0.452 A g^{-1}) current density

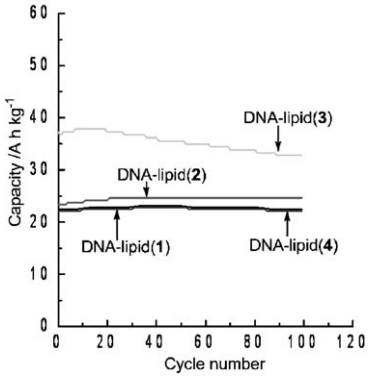

Figure 7. Dependence of capacity on cycle number in DNA–lipid(**1**–**4**). Charge and discharge were repeated at a current density of 0.88 mA cm^{-2} (0.385–0.452 A g^{-1}) in a range of 2.5–4.2 V cell voltage.

in a voltage range of 2.5–4.2 V. The cell with DNA–lipid(**3**) maintained over 90% capacity after 100 cycles. The discharge capacity of DNA–lipid(**1**), DNA–lipid(**2**), and DNA–lipid(**4**) did not change even after 100 cycles. It seems that the cycle life of DNA–lipid(**1**–**4**)-based cells is comparable to or better than that of the reported poly(2,2,6,6-tetramethylpiperidinyloxy-4-yl methacrylate) (PTMA) system.[27]

Conclusion

We have presented in this article the first example of DNA-based secondary battery, and disclosed that the TEMPO-carrying DNA–lipid complexes undergo two-stage redox reaction leading to large capacities. Specifically, we have synthesized novel DNA–lipid complexes that contain TEMPO by replacing the sodium counterion with cationic amphiphilic lipid(**1**–**4**); the actual mole ratios of lipid to phosphate in the products were 0.84:1 to 0.16:1. All the TEMPO-containing DNA–lipid complexes demonstrated reversible multi-stage charge/discharge processes, the discharge capacities of which were 40.5–60.0 A h kg^{-1}. Thus DNA–lipid(**1**–**4**) could be applied to cathode-active materials in the organic radical battery, which features quick charge and discharge, and high power density. In particular, the capacity of a DNA–lipid(**3**)-based cell reached 60.0 A h kg^{-1}, which corresponds to 192% of the theoretical value for the one-electron redox reaction, indicating that a two-electron process takes place.

Experimental Section

Materials: The sodium salt of DNA from salmon testes (>95%) was donated from Japan Chemical Feeding Company, and used without farther purification. According to the data of Japan Chemical Feeding Company, the weight-average molecular weight of the DNA sample is 6.60×10^6 (ca. 30000 bp; tested by electrophoresis). *N*-(3-Dimethylaminopropyl)-*N'*-ethylcarbodiimide hydrochloride (EDC·HCl; Eiweiss), 4-dimethylaminopyridine (DMAP; Wako), 11-bromoundecanoic acid (Aldrich), 12-bromo-1-dodecanol (TCI), 4-hydroxy-TEMPO (TCI), L-glutamic acid-α,γ-dimethyl ester hydrochloride (L-H-Glu(OMe)-OMe·HCl), and N-α-*tert*-butoxycarbonyl-L-glutamic acid (BOC-Glu-OH) (Watanabe Chemical Industries, Ltd) were purchased and used without further purification.

Measurements: ^{1}H (400 MHz) and ^{13}C (100 MHz) NMR spectra were recorded on a JEOL EX-400 spectrometer by using tetramethylsilane as an internal standard. Broad-line NMR and low-frequency ESR spectra were recorded around 50 MHz with a homebuilt spectrometer to estimate a spin number in a unit. Spin densities were estimated by a Quantum Design MPMS susceptometer. ESR spectra to determine the *g* factors were measured with JEOL X-band (9.48 GHz) spectrometer with a frequency counter (Anritsu, MF76 A) and an NMR field meter (Echo Electronics, EFM-2000 AX). IR spectra were measured on a JASCO FT/IR-4100, CD and UV/Vis spectra were recorded on a JASCO J-800 specrtropolarimeter. Elemental analysis was carried out at the Kyoto University Elemental Analysis Center. Cyclic voltammograms were measured on an HCH Instruments ALS600 A-n electrochemical analyzer. The measurements were carried out with a glassy carbon rod as a working electrode coupled with a Pt plate counter electrode and an Ag/AgCl reference electrode, with a solution of a polymer (0.5 mg mL^{-1}) and tetrabutylammonium perchlorate (TBAP, 0.1 M) in $CHCl_3$. Thermal gravimetric analysis (TGA) was carried out on a Shimadzu TGA-50 thermal analyzer. The content of Na ion was determined by inductively coupled plasma (ICP) emission spectrometry using a Shimadzu ICP-1000 IV spectrometer; DNA–lipid samples were dissolved in 2 N HCl.

Synthesis of lipids: Lipid(**4**), which contains both TEMPO radicals and an amino acid dendrimer (G2), was synthesized by the route illustrated in Scheme 1. The synthetic routes of lipid(**1**–**3**) were similar to that of lipid(**4**). The experimental procedures for the synthesis of lipid(**4**) are detailed below as an example.

Preparation of compound 8: L-H-Glu(OMe)-OMe·HCl (5.0 g, 14.4 mmol) was added to a solution of EDC·HCl (2.80 g, 14.4 mmol) and DMAP (175 mg, 1.44 mmol) in CH_2Cl_2 (80 mL) at room temperature. BOC-Glu-OH (1.75 mg, 7.2 mmol) was added to the solution, and the resulting mixture was stirred at room temperature overnight. The reaction

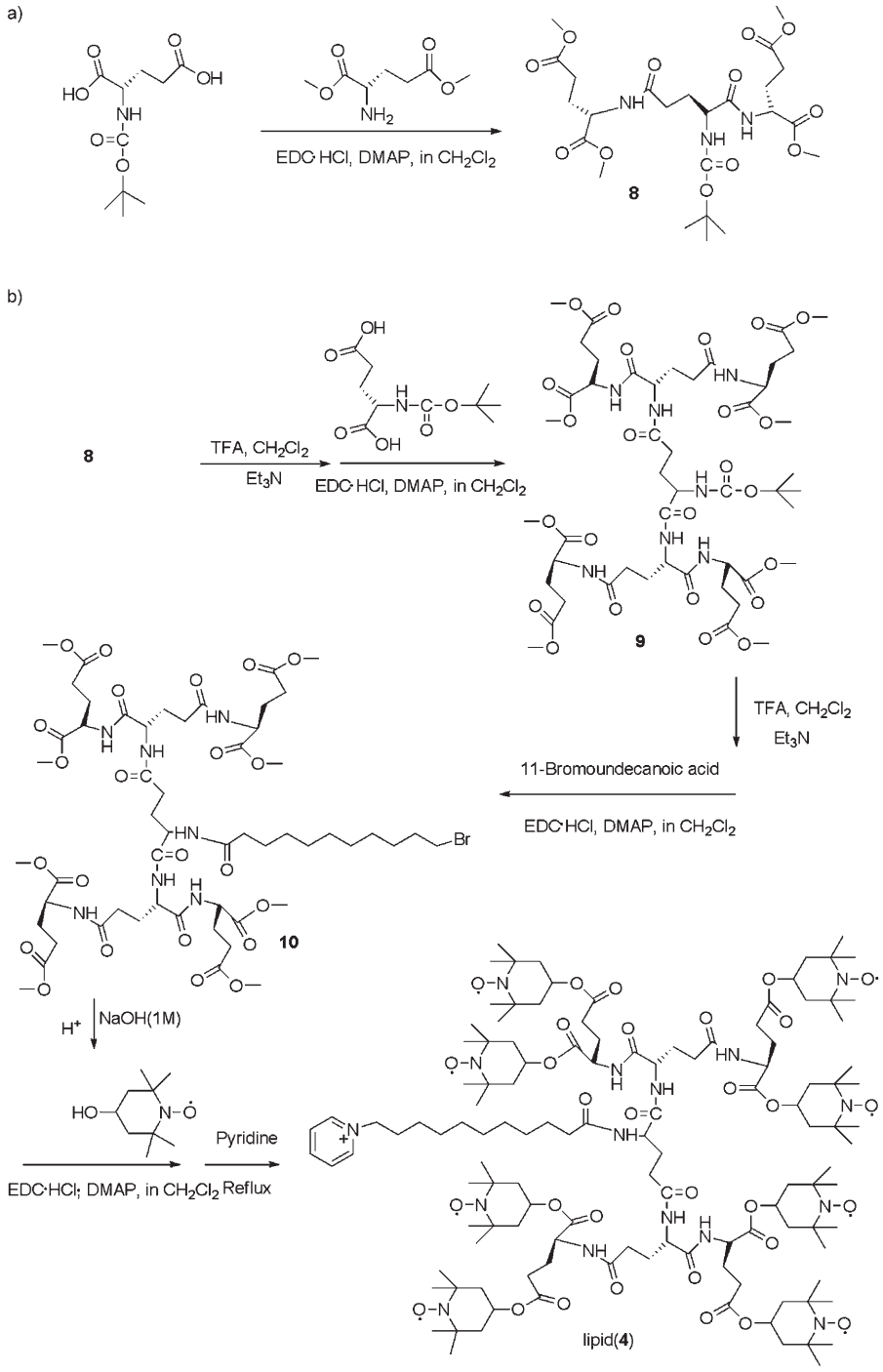

Scheme 1. Synthetic route of lipid(**4**).

mixture was washed with water (50 mL) three times, and the organic layer was dried over anhydrous $MgSO_4$. After filtration, the solvent was removed by rotary evaporation to afford the crude product. It was purified passing a silica gel column with a $CHCl_3$/ethanol mixture (9:1 volume ratio) as eluent. A white solid of **5** was obtained in 80% yield (4.06 g). ^{1}H NMR ($CDCl_3$): $\delta = 1.39$ (s, 9H; -COOC(CH_3)$_3$), 2.04–2.06 (m, 4H; -NHCOCH_2CH_2CH), 2.43–2.47 (m, 8H; 2CHCH_2CH_2COOMe), 3.67–3.72 (m, 12H; 4COO*Me*), 4.50–4.59 ppm (m, 3H; 3NHC*H*-(CH_2)COO); ^{13}C NMR ($CDCl_3$): $\delta = 26.4$, 26.6, 30.1, 30.4, 30.7, 33.4, 51.9, 54.3, 79.5, 158.7, 172.5, 172.9, 174.7 ppm.

Preparation of compound 9: The *N*-*tert*-butyloxycarbonyl group of compound **8** was removed according to the literature,[33] and then the product was reacted with BOC-Glu-OH in a manner similar to the synthesis of **8**. Yield 65%; white solid; ^{1}H NMR ($CDCl_3$): $\delta = 1.39$ (s, 9H; -COOC-(CH_3)$_3$), 2.09–2.12 (m, 12H; 3NHCOCH_2CH_2CH); 2.41–2.45 (m, 16H; 4CHCH_2CH_2COOMe), 3.60–3.62 (m, 24H; 8COO*Me*), 4.50–4.55 (m, 7H; 7NHC*H*(CH_2)COO), 8.32–8.36 ppm (br, 7H; 7N*H*); ^{13}C NMR ($CDCl_3$): $\delta = 26.4$, 26.6, 27.6, 28.6, 30.0, 51.6, 54.3, 79.6, 155.7, 172.5, 172.9, 173.0 ppm.

Preparation of compound 10: The *N*-*tert*-butyloxycarbonyl group of compound **9** (1.80 g, 1.58 mmol) was removed according to the literature,[33] and then the product was added to a solution of EDC·HCl (0.4 g, 2.0 mmol), DMAP (24 mg, 0.30 mmol) and 11-bromoundecanoic acid (0.53 g, 2.0 mmol) in CH_2Cl_2 (45 mL) at room temperature. The resulting mixture was stirred at room temperature overnight. The reaction mixture was washed with water (50 mL) three times, and the organic layer was dried over anhydrous $MgSO_4$. It was filtered, and the filtrate was concentrated on a rotary evaporator. The residual mass was purified by silica gel column chromatography eluted with *n*-hexane/ethyl acetate = 4:1 (volume ratio) to give **10** as a white solid. Yield 1.25 g (63%); ^{1}H NMR (400 MHz, $CDCl_3$): $\delta = 1.29$–2.04 (m, 18H; -(CH_2)$_9$$CH_2$Br), 2.05–2.09 (m, 12H; 3NHCOCH_2CH_2CH), 2.27–2.31 (m, 16H; 4CHCH_2CH_2COOMe), 3.31–3.34 (m, 2H; CH_2Br), 3.67–3.69 (m, 24H; 8COO*Me*), 4.60–4.64 (m, 7H; 7NHC*H*(CH_2)COO), 8.30–8.41 ppm (br, 7H; 7N*H*); ^{13}C NMR ($CDCl_3$): $\delta = 24.1$, 24.6, 28.0, 28.6, 28.7, 28.9, 29.0, 29.1, 29.2, 32.7, 33.9, 35.1, 51.9, 52.8, 54.2, 169.6, 171.9, 172.0, 172.1, 172.7, 172.9, 173.4 ppm.

Preparation of lipid(4): The methyl group of compound **10** was removed according to the literature,[33] and then the product was treated with 4-hydroxy-TEMPO in a manner similar to the synthesis of compound **8**. Yield 80%; orange-red liquid. The product was then dissolved in pyridine (50 mL) and stirred at reflux temperature for 2 days. After cooling to room temperature, the reaction mixture was concentrated on a rotary evaporator, and then washed with diethyl ether and dried in a vacuum oven at 50 °C for 6 days; eventually the brown-red liquid lipid(**4**) was obtained. Yield 1.0 g (61%, 2.0 mmol); IR (KBr): $\tilde{\nu} =$ 3417, 2973, 2931, 2857, 1732, 1635, 1489, 1465, 1362, 1315, 1238, 1173, 1111, 1014, 775, 687, 559, 482 cm^{-1}; elemental analysis calcd (%) for $C_{124}H_{207}N_{16}O_{31}Br$: C 59.62, H 8.35, N 8.97; found: C 59.16, H 8.62, N 9.23.

Preparation of lipid(4): Lipid(**1**) was synthesized from 11-bromoundecanoic acid and 4-hydroxy-TEMPO in a manner similar to compound **8**,

followed by the reaction with pyridine in a manner similar to Lipid(**4**). Yield 80%; orange-red liquid; IR (KBr): $\tilde{\nu}$=3421, 2973, 2931, 2858, 1732, 1635, 1489, 1465, 1365, 1315, 1238, 1173, 1110, 1052, 1014, 775, 687, 559, 486 cm^{-1}; elemental analysis calcd (%) for $C_{26}H_{45}O_3BrN_2$: C 60.81, H 8.83, N 5.45; found: C 60.50, H 8.59, N 5.30.

Preparation of lipid(2): Lipid(**2**) was synthesized in a manner similar to lipid(**4**). Yield 80%; orange-red liquid; IR (KBr): $\tilde{\nu}$=3425, 2974, 2931, 2858, 1732, 1635, 1489, 1465, 1365, 1315, 1238, 1173, 1110, 1049, 1014, 775, 687, 559, 478 cm^{-1}; elemental analysis calcd (%) for $C_{40}H_{69}O_7N_4Br$: C 60.41, H 8.72, N 7.02; found: C 60.50, H 8.59, N 7.30.

Preparation of lipid(3): Lipid(**3**) was prepared in a manner similar to lipid(**4**). Yield 82%; orange-red liquid; IR (KBr): $\tilde{\nu}$=3421, 2973, 2931, 2858, 1732, 1635, 1489, 1466, 1365, 1315, 1238, 1173, 1111, 1053, 1014, 987, 775, 687, 559, 482 cm^{-1}; elemental analysis calcd (%) for $C_{68}H_{115}N_8O_{15}Br$: C 59.85, H 8.49, N 8.21; found: C 60.01, H 8.32, N 8.61.

Preparation of DNA–lipid complexes:[34,35] A small amount of lipid (2.0 mmol) in THF was added slowly into double-distilled H_2O to form a uniform solution. An aqueous solution (200 mL) of DNA–Na from salmon testes (0.50 g) was added dropwise into an aqueous lipid solution (the feed mole ratio of lipid to phosphate was 1.50). Immediately, the DNA–lipid complex precipitated out from the aqueous solution. After stirring for 24 h, the precipitate was collected by filtration, washed with H_2O to remove free DNA, and then dried in a vacuum oven at 50°C for 24 h. The white DNA–lipid complex was dissolved in chloroform and reprecipitated in THF two times. The obtained DNA–lipid complex was subjected to elemental analysis to determine the actual composition of phosphate anion and the cationic lipid in the DNA–lipid complex.

*Data for DNA–lipid(**1**)*: IR (KBr): $\tilde{\nu}$=3440, 2931, 2857, 1732, 1639, 1489, 1369, 1238, 1173, 1095, 968, 779, 682, 482 cm^{-1}; elemental analysis calcd (%) for DNA–lipid(**1**) complexes with 1:1 ratio of phosphate anion to cationic lipid(**1**): C 56.60, H 7.61, N 10.62, P 4.08; found: C 56.25, H 7.19, N 10.54, P 4.15.

*Data for DNA–lipid(**2**)*: IR (KBr): $\tilde{\nu}$=3440, 2931, 2858, 1744, 1646, 1489, 1365, 1238, 1173, 1091, 964, 883, 821, 786, 728, 686, 520 cm^{-1}; elemental analysis calcd (%) for DNA–lipid(**2**) complexes with 1:1 ratio of phosphate anion to cationic lipid(**2**): C 57.29, H 7.85, N 10.41, P 2.97; found: C 53.49, H 7.41, N 10.41, P 3.89.

*Data for DNA–lipid(**3**)*: IR (KBr): $\tilde{\nu}$=3432, 2931, 2858, 1744, 1635, 1465, 1369, 1273, 1168, 1091, 960, 810, 682, 522 cm^{-1}; elemental analysis calcd (%) for DNA–lipid(**3**) complexes with 1:1 ratio of phosphate anion to cationic lipid(**3**): C 58.02, H 7.97, N 10.22, P 1.92; found: C 55.67, H 7.78, N 10.46, P 3.85.

*Data for DNA–lipid(**4**)*: IR (KBr): $\tilde{\nu}$=3413, 2931, 2857, 1732, 1693, 1647, 1489, 1365, 1242, 1173, 1061, 960, 883, 821, 779, 682, 524 cm^{-1}; elemental analysis calcd (%) for DNA–lipid(**4**) complexes with 1:1 ratio of phosphate anion to cationic lipid(**4**): C 58.57, H 8.05, N 10.09, P 1.13; found: C 55.05, H 7.64, N 10.53, P 4.02.

Determination of the yields of DNA–lipid complexes: We define the yield (%) of a DNA–lipid complex as the ratio of the actual weight of the reaction product to its theoretical weight based on DNA–Na. The yields of DNA–lipid complexes were calculated based on Equation (2)

$$\text{Yield} = \frac{W_{\text{DNA-lipid}} \times 100}{W_{\text{DNA-Na}}\left(1 + \frac{M_{\text{lipid}} - M_{\text{NaBr}}}{M_{\text{base}}}\right)} \quad (2)$$

in which $W_{\text{DNA-lipid}}$ is the actual weight of DNA–lipid complex, $W_{\text{DNA-Na}}$ is the feed weight of DNA–Na, M_{lipid} and M_{NaBr} are the molecular weights of lipid and NaBr, respectively, and M_{base} is the average molecular weight of base groups in the repeating unit of DNA–Na [the value is 347.91 calculated from the structures of base couple (according to the fragment sequence of salmon DNA with an AT/GC ratio of approximately 56:44)].[36]

Determination of the mole ratios of lipid/phosphate and TEMPO/phosphate in DNA–lipid complexes: The actual mole ratios of lipid to phosphate ($R_{\text{l/p}}$) in the DNA–lipid complexes were estimated from the amounts of phosphorus before and after complexation. The amount of phosphorus was determined by elemental analysis. The actual percent phosphorus content in a DNA–lipid ($P_{\text{DNA-lipid}}$) was calculated based on Equation (3) for the percent phosphorus:

$$P_{\text{DNA-lipid}} = \frac{P_{\text{DNA-Na}}}{1 + \frac{R_{\text{l/p}}(M_{\text{lipid}} - M_{\text{NaBr}})}{M_{\text{base}}}} \quad (3)$$

in which $P_{\text{DNA-Na}}$ is the percent phosphorus content in DNA–Na (the value was 8.50% according to elemental analysis), $R_{\text{l/p}}$ is the actual mole ratio of lipid to phosphate in the DNA–lipid complexes, and the definitions of M_{lipid}, M_{NaBr}, and M_{base} are the same as for Equation (2). When solved for $R_{\text{l/p}}$, we get Equation (4). The mole ratio of TEMPO/phosphate ($R_{\text{t/p}}$) in the DNA–lipid complexes was estimated from Equation (5) in which m is the number of TEMPO moieties in a lipid.

$$R_{\text{l/p}} = \frac{(P_{\text{DNA-Na}} - P_{\text{DNA-lipid}}) \times M_{\text{base}}}{P_{\text{DNA-lipid}} \times (M_{\text{lipid}} - M_{\text{NaBr}})} \quad (4)$$

$$R_{\text{t/p}} = R_{\text{l/p}}\, m \quad (5)$$

Determination of spin number, spin density, and the mole ratio of TEMPO radical/phosphate: The spin density (D_{S}; spin g^{-1}) was obtained by SQUID, the values of which are listed in Table 2, and then spin number (N_{S}; spin/unit) in a lipid was calculated from D_{S} by using Equation (6)in which N_{A} is the Avogadro's number, and M is the actual molecular weight expressed by the Equation (7). Apart from this, N_{S} was independently determined by ESR spectroscopy, and then their average value $\langle N_{\text{S}} \rangle$ was obtained. The mole ratio of TEMPO radical/phosphate ($R_{\text{r/p}}$) was calculated based on Equation (8).

$$N_{\text{S}} = D_{\text{S}}\,(M/N_{\text{A}}) \quad (6)$$

$$M = R_{\text{l/p}}\, M_{\text{lipid}} + M_{\text{base}} \quad (7)$$

$$R_{\text{r/p}} = R_{\text{t/p}}\,\langle N_{\text{S}} \rangle / m = R_{\text{l/p}}\,\langle N_{\text{S}} \rangle \quad (8)$$

Fabrication and electrochemical measurements of batteries using the DNA–lipid complexes: A coin-type cell was fabricated by stacking electrodes (1.13 cm^2) with porous polyolefin separator films. A cathode was formed by pressing the composites of a DNA–lipid complex (10 wt%), carbon fiber (80 wt%), and fluorinated polyolefin binder (10 wt%) as described in a previous paper.[29] The cathode was set to a coin-type cell possessing a lithium metal anode. A composite solution of ethylene carbonate (30 vol%)/diethyl carbonate (70 vol%) containing 1 M of $LiPF_6$ was used as an electrolyte. Charge/discharge properties were measured at 25°C by using a computer-controlled automatic battery charge and discharge instrument (Keisokukiki, Battery Labo System BLS5500). The theoretical capacity (C_{th}; A h kg^{-1}) of an electroactive complex was calculated from the spin density N_{S} (per gram) in the complex [Eq. (9)].[16]

$$C_{\text{th}} = \frac{D_{\text{s}}\, 1.602 \times 10^{-19}}{3600/1000} \quad (9)$$

Acknowledgements

We would like to thank Professor Y. Okahata at Tokyo Institute of Technology for helpful discussion. This research was supported in part by a grant program "Collaborative Development of Innovative Seeds" from the Japan Science and Technology Agency. Thanks are also due to the Iketani Science and Technology Foundation for financial support. J.Q. ac-

knowledges the financial support from the Ministry of Education, Culture, Sports, Science, and Technology (Monbukagakusho), Japan.

[1] E. R. Kay, D. A. Leigh, F. Zerbetto, *Angew. Chem.* **2007**, *119*, 72–196; *Angew. Chem. Int. Ed.* **2007**, *46*, 72–191.
[2] U. Feldkamp, C. M. Niemeyer, *Angew. Chem.* **2006**, *118*, 1888–1910; *Angew. Chem. Int. Ed.* **2006**, *45*, 1856–1876.
[3] N. L. Rosi, C. A. Mirkin, *Chem. Rev.* **2005**, *105*, 1547- 1562.
[4] K. Kinbara, T. Aida, *Chem. Rev.* **2005**, *105*, 1377–1400.
[5] N. C. Seeman, *Nature* **2003**, *421*, 427–431.
[6] M. H. Caruthers, *Science* **1985**, *230*, 281–285.
[7] I. Koltover, T. Salditt, J. O. Rädler, C. R. Safinya, *Science* **1998**, *281*, 78–81.
[8] J. O. Rädler, I. Koltover, T. Salditt, C. Safinya, *Science* **1997**, *275*, 810–814.
[9] M. S. Spector, J. M. Schnur, *Science* **1997**, *275*, 791–792.
[10] L. Cui, J. Miao, L. Zhu, *Macromolecules* **2006**, *39*, 2536–2545.
[11] A. Joy, A. K. Ghosh, G. B. Schuster, *J. Am. Chem. Soc.* **2006**, *128*, 5346–5347.
[12] Y. Kawabe, L. Wang, S. Horinouchi, N. Ogata, *Adv. Mater.* **2000**, *12*, 1281–1283.
[13] W. L. Hsu, H. L. Chen, W. Liou, H. K. Lin, W. L. Liu, *Langmuir* **2005**, *21*, 9426–9431.
[14] M. F. Ottaviani, E. Cossu, N. J. Turro, D. A. Tomalia, *J. Am. Chem. Soc.* **1995**, *117*, 4387–4398.
[15] V. W. Bowry, K. U. Ingold, *J. Am. Chem. Soc.* **1992**, *114*, 4992–4996.
[16] W. Adam, C. R. Saha-Möller, P. A. Ganeshpure, *Chem. Rev.* **2001**, *101*, 3499–3548.
[17] I. Streeter, A. J. Wain, M. Thompson, R. G. Compton, *J. Phys. Chem. A* **2005**, *109*, 12636–12649.
[18] Y. Miwa, K. Yamamoto, M. Sakaguchi, M. Sakai, K. Tanida, S. Hara, S. Okamoto, S. Shimada, *Macromolecules* **2004**, *37*, 831–839.
[19] Z. Veksli, W. G. Miller, *Macromolecules* **1977**, *10*, 686–692.
[20] T. Iwamoto, H. Masuda, S. Ishida, C. Kabuto, M. Kira, *J. Am. Chem. Soc.* **2003**, *125*, 9300–9301.
[21] C. D. Anderson, K. J. Shea, S. D. Rychnovsky, *Org. Lett.* **2005**, *7*, 4879–4882.
[22] P. Ferreira, E. Phillips, D. Rippon, S. C. Tsang, W. Hayes, *J. Org. Chem.* **2004**, *69*, 6851–6859.
[23] K. Nakahara, J. Iriyama, S. Iwasa, M. Suguro, M. Satoh, E. J. Cairns, *J. Power Sources* **2007**, *163*, 1110–1113.
[24] K. Nakahara, S. Iwasa, J. Iriyama, Y. Morioka, M. Suguro, M. Satoh, E. Cairns, J. *Electrochim. Acta* **2006**, *52*, 921–927.
[25] H. Nishide, T. Suga, *Electrochem. Soc. Interface* **2005**, *14*, 32–36.
[26] H. Nishide, S. Iwasa, Y. J. Pu, T. Suga, K. Nakahara, M. Satoh, *Electrochim. Acta* **2004**, *50*, 827–831.
[27] K. Nakahara, S. Iwasa, M. Satoh, Y. Morioka, J. Iriyama, M. Suguro, E. Hasegawa, *Chem. Phys. Lett.* **2002**, *359*, 351–354.
[28] J. Qu, T. Katsumata, M. Satoh, J. Wada, J. Igarashi, K. Mizoguchi, T. Masuda, *Chem. Eur. J.* **2007**, *13*, 7965–7973.
[29] J. Qu, T. Katsumata, M. Satoh, J. Wada, T. Masuda, *Macromolecules* **2007**, *40*, 3136–3144.
[30] T. Katsumata, M. Satoh, J. Wada, M. Shiotsuki, F. Sanda, T. Masuda, *Macromol. Rapid Commun.* **2006**, *27*, 1206–1211.
[31] A. Capiomont, B. Chion, J. Lajzerowicz-Bonneteau, H. Lemaire, *J. Chem. Phys.* **1974**, *60*, 2530–2535.
[32] K. Mizoguchi, *Jpn. J. Appl. Phys. Part 1* **1995**, *34*, 1–19.
[33] Y. Li, Q. Li, F. Li, H. Zhang, L. Jia, J. Yu, Q. Fang, A. Cao, *Biomacromolecules* **2006**, *7*, 224–231.
[34] L. Wang, J. Yoshida, N. Ogata, S. Sasaki, T. Kajiyama, *Chem. Mater.* **2001**, *13*, 1273–1281.
[35] Y. Ebara, K. Mizutani, Y. Okahata, *Langmuir* **2000**, *16*, 2416–2418.
[36] G. H. Dixon, M. Smith, *Prog. Nucleic Acid Res. Mol. Biol.* **1968**, *8*, 9–34.

Received: January 7, 2008
Published online: March 13, 2008

